

Peripheral octa-substituted metal-free, cobalt(II) and zinc(II) phthalocyanines bearing coumarin and chloro groups: Synthesis, characterization, spectral and electrochemical properties

Selçuk Altun, Ali Rıza Özkaya*, Mustafa Bulut*

Department of Chemistry, Marmara University, 34722 Göztepe, Kadıköy, Istanbul, Turkey

ARTICLE INFO

Article history:

Received 15 May 2012

Accepted 21 August 2012

Available online 12 September 2012

Keywords:

Coumarin

Phthalocyanine

Octa-substitute

Aggregation

Electrochemistry

ABSTRACT

Novel octa-substituted metal-free, cobalt(II) and zinc(II) phthalocyanines have been synthesized by using chloro and/or coumarin substituted phthalonitrile derivatives. The compounds were characterized by UV–Vis, IR, ¹H NMR, and MALDI–TOF mass spectrometry and elemental analysis. The effects of substituents, metals, solvents and concentration on spectroscopic properties and aggregation behaviour of the novel Pcs were investigated. Furthermore, the redox properties of the octa-4-(4-methoxyphenyl)-7-oxo-8-methylcoumarin-substituted compounds were examined in dimethylsulfoxide and dichloromethane by voltammetry and *in situ* spectroelectrochemistry. Metal-free phthalocyanine and zinc phthalocyanine displayed ligand-based one-electron redox processes whereas cobalt phthalocyanine showed both ligand- and metal-based processes. A couple corresponding to the reduction of 4-(4-methoxyphenyl)-7-oxo-8-methylcoumarin substituents was also detected. The redox processes of the compounds in dimethylsulfoxide were observed to be broad or split, due to the association of electron transfer processes by aggregation–deaggregation equilibrium.

© 2012 Elsevier Ltd. All rights reserved.

1. Introduction

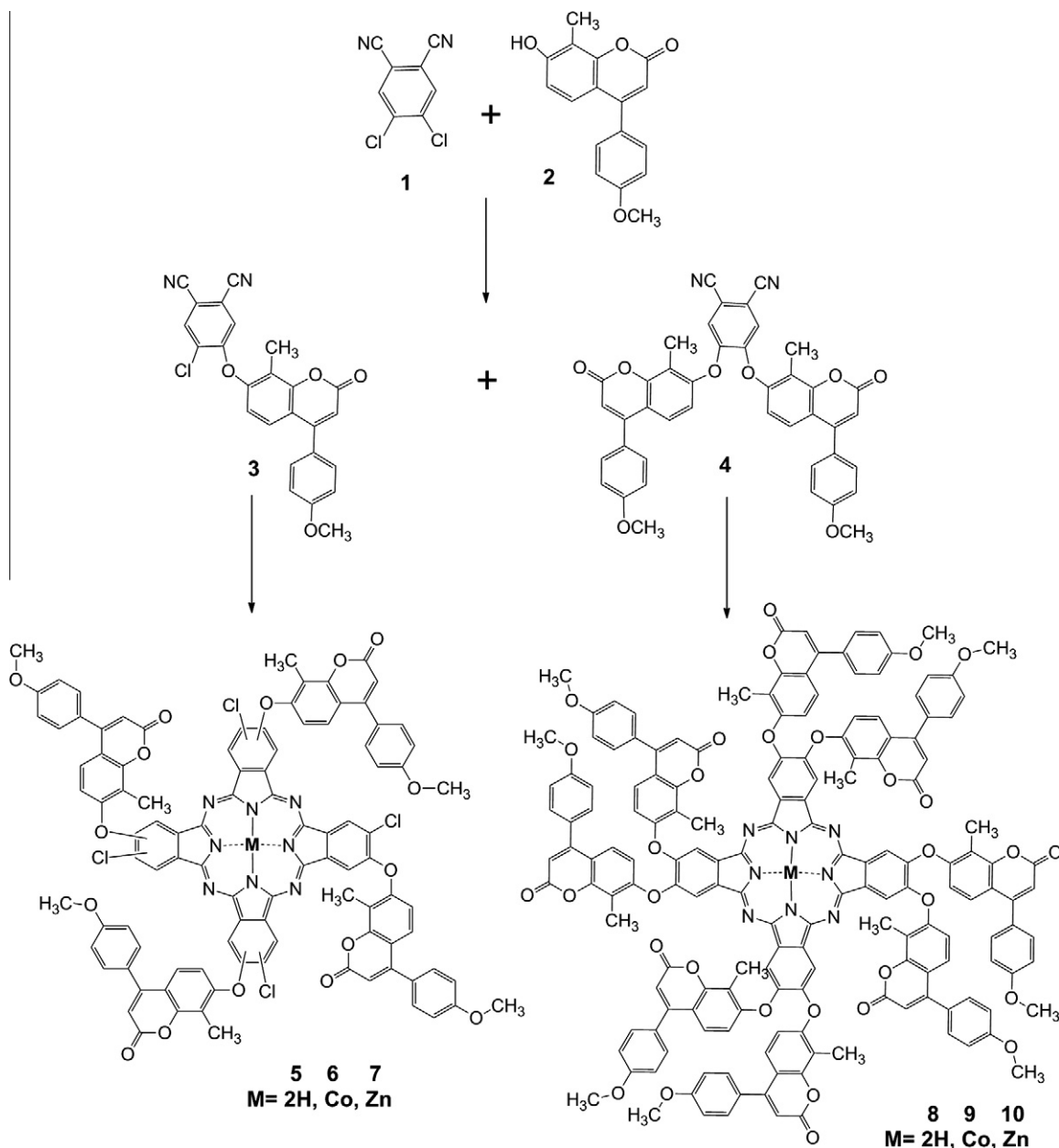
Phthalocyanines (Pcs) form an important class of macrocyclic compounds [1–3] and continue to attract considerable interest as pigments [4], dyes [4], sensors [5,6], photodynamic therapy sensitizers [7–12], optical recording and nonlinear optical materials [13,14], photovoltaics [15], catalysts [16] and electronic device components [17–19]. Due to the growing interest in the properties of metal Pcs, the synthesis of new examples involving various functional substituents, with the aim of modifying their properties in the applications listed above, has become necessary. Coumarin (2H-1-benzopyran-2-one) and its derivatives, found naturally in many higher plants and essential oils including tonka beans, sweet clover and lavender [20,21], are used as anticoagulants [22], additives in food and cosmetics, in the preparation of insecticides, optical brighteners and dispersed fluorescent, laser dyes [23–25], anti-HIV activities, etc. [26]. The family of functional Pcs has been an interesting target for chemists for the development of further chemical reactions on Pc complexes [27–31]. Therefore, we have combined these two functional materials into a single compound via synthetic methodology to obtain novel Pcs bearing different substituents and metals.

Pc compounds have high tendency of aggregation, which is usually depicted as a coplanar association of rings progressing from monomer to dimer and higher order complexes. It is dependent on the concentration, nature of the solvent, peripheral substituents, metal ions and temperature [32,33]. In the aggregated state, the electronic structure of the Pc rings is perturbed resulting in alternation of the ground and excited state electronic structure [34].

In the present work, octa-substituted Pcs bearing only one type of substituent (4-(4-methoxyphenyl)-7-oxo-8-methylcoumarin) **8–10** and both 4-(4-methoxyphenyl)-7-oxo-8-methylcoumarin and chloro substituents **5–7** were synthesized purely and characterized by UV–Vis, IR and MALDI–TOF mass spectrometry, and elemental analysis (Scheme 1). The effect of these substituents as well as the central metal (Co and Zn), solvent (dimethylsulfoxide (DMSO), dichloromethane (DCM), toluene and chloroform) and concentration on the spectroscopic properties and aggregation behaviours of the novel Pcs was also investigated. The understanding of the redox properties of the Pc complexes is important in terms of their applications in many areas. The redox or electron transfer processes of these complexes occur at either the Pc ring or the metal center, depending on the central metal and/or the solvent medium. However, in most cases, it is not possible to distinguish such processes by voltammetry alone. *In situ* spectroelectrochemistry provide additional support for the assignment of these redox processes. Moreover, it is also important in identifying the effect of aggregation–deaggregation equilibrium of Pcs on their redox

* Corresponding authors. Tel.: +90 216 347 96 41; fax: +90 216 347 87 83.

E-mail addresses: aliozkaya@marmara.edu.tr (A.R. Özkaya), mbulut@marmara.edu.tr (M. Bulut).



Scheme 1. Synthesis of starting materials (**3** and **4**) and Pcs (**5**–**10**).

behaviour. Therefore, the electrochemical and *in situ* spectroelectrochemical behaviour of the synthesized Pc complexes were also examined.

2. Experimental

2.1. Material and methods

IR Spectra and electronic spectra were recorded on a Shimadzu FTIR-8300 (KBr pellet) and Shimadzu UV-1601 spectrophotometer, respectively. Elemental analyses were performed by the Instrumental Analysis Laboratory of Tubitak–Ankara. ^1H NMR and ^{13}C NMR spectra were recorded in *d*-chloroform with an instrument Mercury-Vx 400 MHz. Mass spectra were acquired on Autoflex III MALDI-TOF mass spectrometer (Bruker Daltonics, Germany) equipped with a nitrogen UV-laser operating at 337 nm. Spectra were recorded in reflectron mode with average of 50 shots.

2.2. Sample and matrix preparation

α -Cyano-4-hydroxycinnamic acid (ACCA) was prepared in tetrahydrofuran (THF) at a concentration of 10 mg/mL as matrix. MALDI samples were prepared by mixing sample solutions (2 mg/mL in chloroform) and matrix solution (1:10 v/v) in a 0.5 mL Eppendorf® micro tube. Finally, 0.5 μL of this mixture was deposited on the sample plate, dried at room temperature, and then analyzed.

2.3. Synthesis

2.3.1. 4-Chloro-5-(4-(4-methoxyphenyl)-8-methyl-coumarin-7-yloxy)phthalonitrile **3** and 4,5-bis(4-(4-methoxyphenyl)-8-methyl-coumarin-7-yloxy) phthalonitrile **4**

4,5-Dichlorophthalonitrile **1** (1.00 g, 5.08 mmol) and 7-hydroxy-4-(4-methoxyphenyl)-8-methylcoumarin **2** (5.73 g, 20.32 mmol)

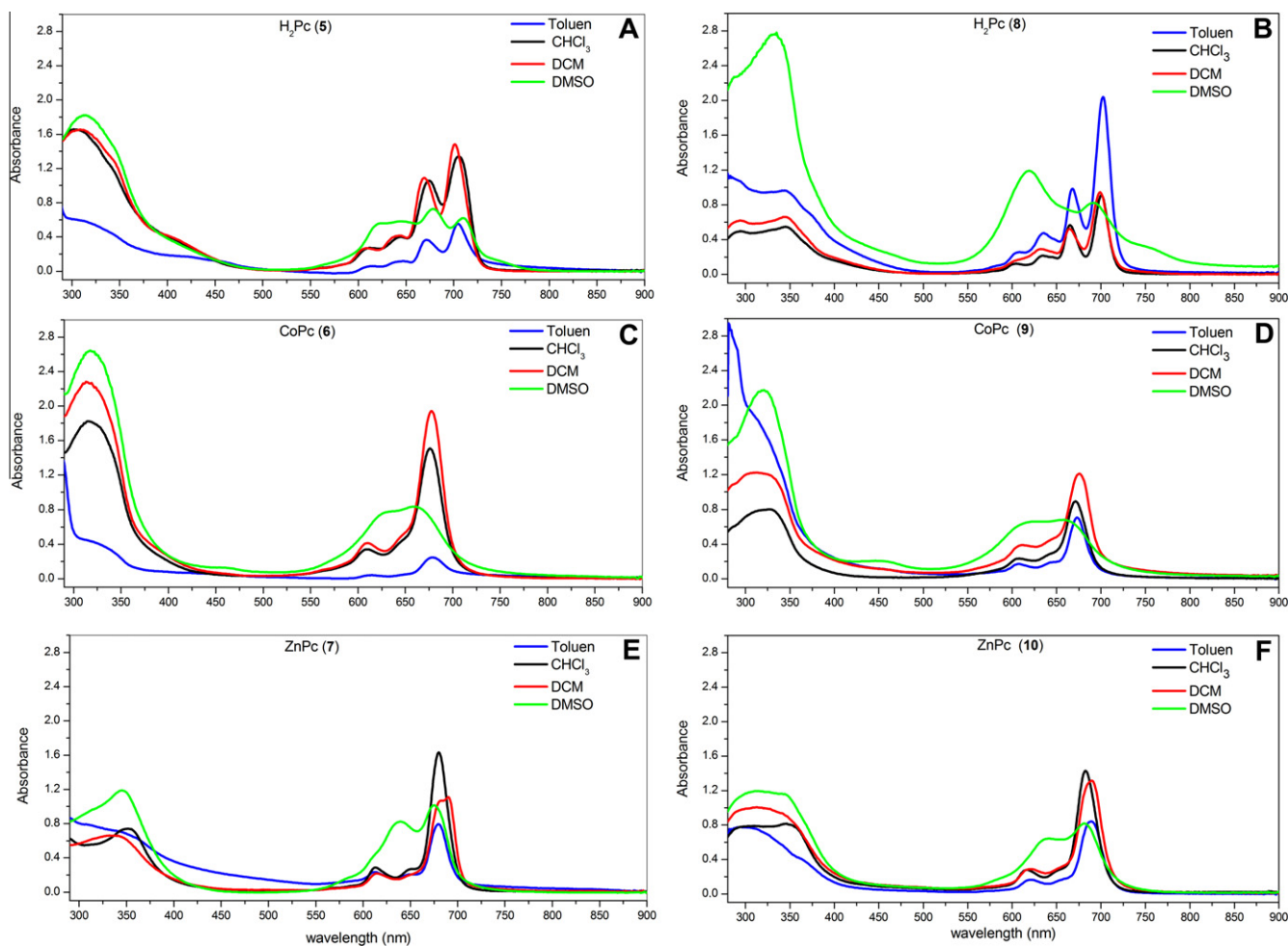


Fig. 1. The UV-Vis spectra of (A) **5**, (B) **6**, (C) **7**, (D) **8**, (E) **9** and (F) **10** in various solvents at 3.0×10^{-6} mol dm $^{-3}$.

were dissolved in anhydrous dimethylformamide (DMF) (30 mL) under N₂ atmosphere. After stirring for 10 min, finely ground anhydrous K₂CO₃ (3.50 g, 25.37 mmol) was added by stirring. The reaction mixture was stirred at 50 °C for 10 days under N₂ atmosphere. Then the mixture was poured in 250 ml cold aqueous solution of 5% HCl. The formed precipitate was filtered off and washed with water. After drying in vacuum at 50 °C, the crude product was purified by column chromatography with silica gel eluting with DCM. Firstly, compound **3** and then compound **4** were obtained purely by using DCM and chloroform as eluting solvents, respectively.

Compound **3** is soluble in DCM, chloroform, THF, DMF and DMSO. Mp: 194–196 °C. Yield: 1.30 g (58.04%). *Anal. Calc.* for C₂₅H₁₅ClN₂O₄: C, 67.80; H, 3.41; N, 6.33. Found: C, 68.02; H 3.31; N, 6.42%. IR (KBr pellet) ν_{\max} (cm $^{-1}$): 530, 742, 826, 956, 1079, 1175, 1245, 1482, 1511, 1578, 1603, 1720, 2235, 2838, 2930, 3025, 3096. ¹H NMR (CDCl₃): δ , ppm: 2.20 (s, 3H), 3.75 (s, 3H), 6.71 (*d*, *J* = 8.59 Hz, 1H), 6.87 (s, 1H), 6.91 (*dd*, *J* = 8.59 Hz and *J* = 2.74 Hz, 2H), 7.27 (*dd*, *J* = 8.59 Hz and *J* = 2.73 Hz, 2H), 7.35 (*d*, *J* = 8.98 Hz, 1H), 7.77 (s, 1H), 7.15 (s, 1H). ¹³C NMR. (CDCl₃), δ , ppm: 161.04, 160.37, 156.75, 155.02, 154.07, 153.61, 135.77, 129.91, 127.21, 126.18, 120.27, 119.44, 117.62, 115.68, 114.48, 114.45, 110.47, 55.65, 9.26.

Compound **4** is soluble in DCM, chloroform, THF, DMF and DMSO. Mp: 175–178 °C. Yield: 0.29 g (8.56%). *Anal. Calc.* for C₄₂H₂₈N₂O₈: C, 73.25; H, 4.10; N 4.07. Found: C, 73.41; H, 3.98; N, 4.19%. IR (KBr pellet) ν_{\max} (cm $^{-1}$): 531, 725, 832, 956, 1081, 1173, 1245, 1292, 1365, 1422, 1499, 1603, 1713, 2232, 2838,

2931, 3042. ¹H NMR (CDCl₃) δ , ppm: 2.20 (s, 6H), 3.74 (s, 6H), 6.70 (*d*, *J* = 8.99 Hz, 2H), 6.90 (*dd*, *J* = 8.99 Hz and *J* = 2.73 Hz, 4H), 7.03 (s, 2H), 7.11 (s, 2H), 7.25 (*dd*, *J* = 8.99 Hz and *J* = 2.73 Hz, 4H), 7.33 (*d*, *J* = 8.59 Hz, 2H). ¹³C NMR (CDCl₃), δ , ppm: 160.95, 160.35, 155.11, 154.30, 153.97, 150.59, 129.91, 127.19, 125.95, 122.14, 118.80, 117.14, 114.85, 114.45, 114.00, 113.99, 111.35, 55.48, 9.00.

2.3.2. General procedure of synthesis of metal-free Pcs **5** and **8**

The compound **3** (0.20 g, 4.52×10^{-4} mol) or compound **4** (0.20 g, 2.90×10^{-4} mol) was heated in 2 ml dry 2-*N,N*-dimethylaminoethanol in a sealed tube. The mixture was held at 160 °C for 48 h under N₂ atmosphere. After cooling to room temperature, the reaction mixture was treated with dilute HCl and the mixture was filtered and washed with water until the filtrate became neutral. The raw green product was taken in the soxhlet apparatus and then purified by washing with acetic acid, water, ethanol and acetonitrile for 12 h respectively. The crude product was purified on column chromatography with silica gel eluting with chloroform a gradient of chloroform-THF from 0% to 5% THF.

2.3.2.1. 2(3),9(10),16(17),23(24)-Tetrachloro-3(2),10(9),17(16),24(23)-tetrakis(4-(4-methoxyphenyl)-8-methylcoumarin-7-yloxy)phthalocyanine **5**. The compound **5** was obtained and purified as mentioned by the procedure above for synthesis of metal-free Pcs. This compound is soluble in toluene, DCM, chloroform, THF, DMF, dimethylacetamide (DMA) and DMSO Mp > 300 °C. Yield: 79.37 mg (58.24%). *Anal. Calc.* for C₁₀₀H₆₂Cl₄N₈O₁₆: C, 67.73; H, 3.52; N, 6.32. Found: C, 67.55; H,

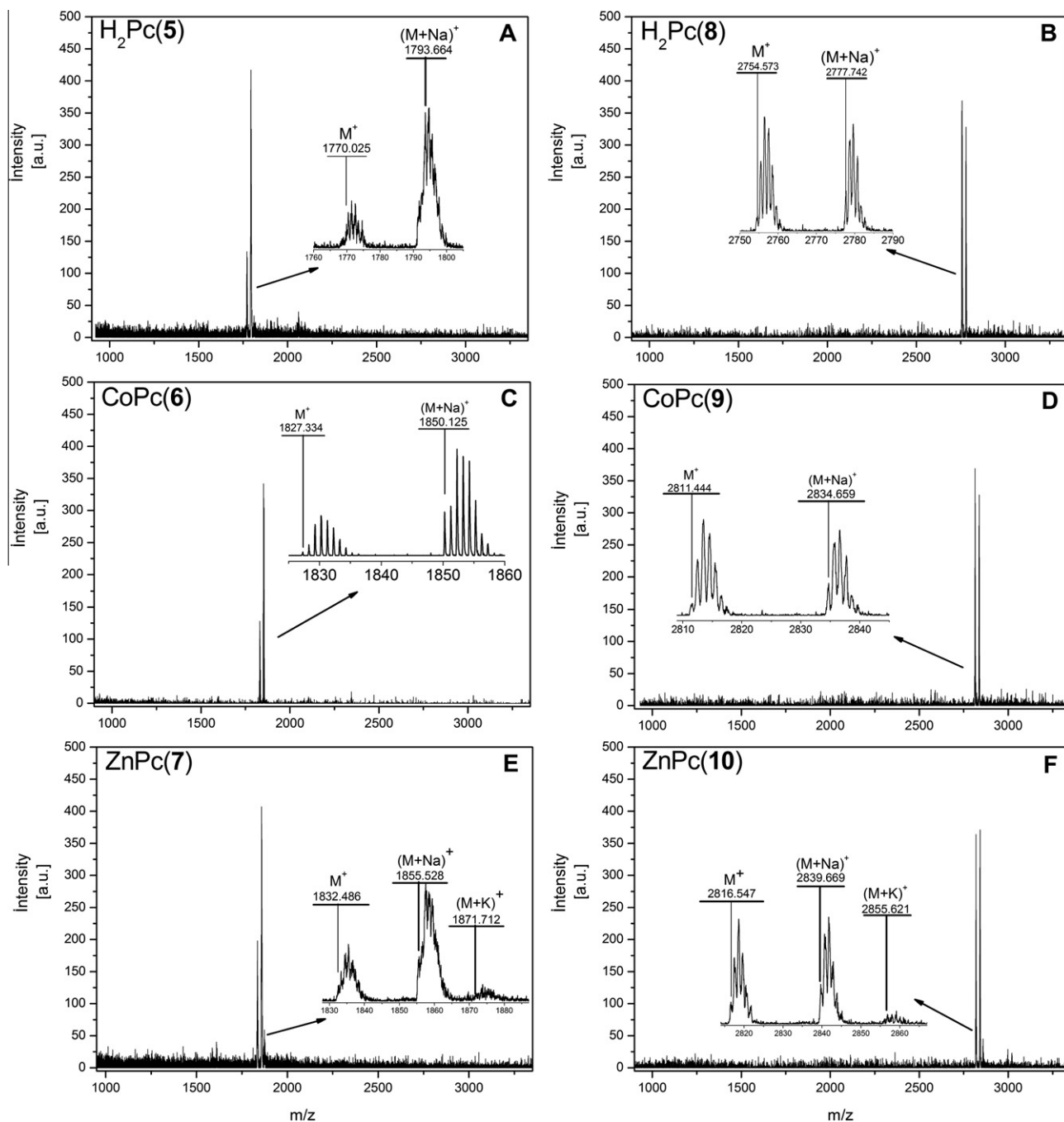


Fig. 2. Positive ion in reflectron mode MALDI-TOF MS spectra of (A) **5**, (B) **8**, (C) **6**, (D) **9** and (E) **7** and (F) **10** in α -cyano-4-hydroxycinnamic acid. Inset spectrum shows expanded molecular ion, sodium and potassium ion adducts mass region of the complex.

3.38; N, 6.46%. IR (KBr pellet) ν_{\max} (cm^{-1}): 534, 614, 760, 836, 883, 960, 1023, 1086, 1177, 1250, 1366, 1440, 1513, 1603, 1645, 1730, 2854, 2924, 2955, 3289. MALDI-TOF mass: m/z 1770.025 (M^+) and 1793.664 ($M+Na^+$). UV-Vis (DCM): λ_{\max} (nm), ($\log \epsilon$): 310 (5.742), 609 (4.954), 644 (5.289), 678 (5.384), 710 (5.732). ^1H NMR. (CDCl_3), δ , ppm: 7.73–6.98 (m, 36H, Ar-H), 3.82 (s, 12H, $\text{CH}_3\text{-O}$), 2.27 (s, 12H, $\text{CH}_3\text{-}$), 1.48 (s, 2H). ^{13}C NMR (CDCl_3), δ , ppm: 160.72, 151.80, 135.75, 135.64, 132.72, 129.99, 127.56, 125.36, 125.05, 114.10, 55.43, 38.01, 34.21, 30.46.

2.3.2.2. *2,3,9,10,16,17,23,24-Octakis(4-(4-methoxy-phenyl)-8-methyl-coumarin-7-yloxy)phthalocyanine 8*. Compound **8** is soluble in toluene, DCM, chloroform, THF, DMF and DMSO. Mp > 300 °C. Yield: 37.27 mg (35.50%). Anal. Calc. for $\text{C}_{168}\text{H}_{114}\text{N}_8\text{O}_{32}$: C, 73.20;

H, 4.17; N, 4.06. Found: C, 73.01; H, 3.99; N, 4.21%. IR (KBr pellet) ν_{\max} (cm^{-1}): 532, 685, 744, 837, 882, 986, 1021, 1085, 1178, 1252, 1367, 1433, 1513, 1599, 1645, 1732, 2841, 2865, 2956, 3073, 3298. MALDI-TOF mass m/z : 2754.573 (M^+), 2777.742 ($M+Na^+$). UV-Vis (DCM): λ_{\max} (nm), ($\log \epsilon$): 295 (5.316), 343 (5.343), 605 (4.732), 632 (4.988), 665 (5.241), 699 (5.498). ^1H NMR (CDCl_3), δ , ppm: 7.74–6.92 (m, 64H, Ar-H), 3.74 (s, 24H, $\text{CH}_3\text{-O}$), 2.64 (s, 24H, $\text{CH}_3\text{-}$), 1.53 (s, 2H).

2.3.3. General procedure of synthesis of metal Pcs **6,7,9** and **10**

A mixture of compound **3** (0.20 g, 4.52×10^{-4} mol) or compound **4** (0.20 g, 2.90×10^{-4} mol) with $\text{Zn}(\text{OAc})_2 \cdot 2\text{H}_2\text{O}$ (0.13 g, 5×10^{-4} mol) or $\text{Co}(\text{OAc})_2 \cdot 4\text{H}_2\text{O}$ (0.09 g, 5×10^{-4} mol) was powdered in a quartz crucible and transferred in a reaction tube.

Table 1
Spectral data for Pcs **5–10** in various solvents at 3.0×10^{-6} mol dm $^{-3}$.

| Solvent | Pcs | Q-band, λ_{\max}/nm | Log ϵ | B-band, λ_{\max}/nm | Log ϵ |
|-------------------|-----------|------------------------------------|----------------------------|------------------------------------|----------------|
| Toluen | 5 | 704, 673, 645, 610 | 5.603, 5.463, 5.143, 5.010 | 303 | 5.654 |
| CHCl ₃ | 5 | 705, 674, 644, 613 | 5.638, 5.547, 5.125, 4.959 | 302 | 5.742 |
| DCM | 5 | 701, 669, 644, 609 | 5.694, 5.561, 5.141, 4.954 | 310 | 5.742 |
| DMSO | 5 | 710, 678, 644, 623 | 5.732, 5.384, 5.289, 5.267 | 312 | 5.784 |
| Toluen | 6 | 679, 615 | 5.099, 4.756 | 309 | 5.292 |
| CHCl ₃ | 6 | 676, 610 | 5.542, 4.905 | 317 | 5.627 |
| DCM | 6 | 678, 610 | 5.504, 4.830 | 315 | 5.573 |
| DMSO | 6 | 659, 629 | 5.357, 5.337 | 319 | 5.694 |
| Toluen | 7 | 679, 652, 612 | 5.372, 4.602, 4.690 | 315 | 5.326 |
| CHCl ₃ | 7 | 680, 651, 613 | 5.525, 4.746, 4.771 | 352 | 5.182 |
| DCM | 7 | 685, 614 | 5.568, 5.024 | 336 | 5.343 |
| DMSO | 7 | 675, 639 | 5.529, 5.438 | 345 | 5.598 |
| Toluen | 8 | 702, 668, 636, 607 | 5.571, 5.258, 5.917, 4.647 | 343 | 5.231 |
| CHCl ₃ | 8 | 700, 665, 635, 605 | 5.481, 5.276, 4.855, 4.613 | 345 | 5.262 |
| DCM | 8 | 699, 665, 632, 605 | 5.498, 5.241, 4.988, 4.732 | 343 | 5.343 |
| DMSO | 8 | 691, 619 | 5.188, 5.323 | 334 | 5.670 |
| Toluen | 9 | 673, 607 | 5.373, 4.758 | 311 | 5.802 |
| CHCl ₃ | 9 | 671, 607 | 5.414, 4.822 | 327 | 5.374 |
| DCM | 9 | 676, 612 | 5.605, 5.113 | 312 | 5.610 |
| DMSO | 9 | 656, 625 | 5.254, 5.212 | 320 | 5.862 |
| Toluen | 10 | 689, 621 | 5.448, 4.735 | 295 | 5.413 |
| CHCl ₃ | 10 | 682, 617 | 5.673, 4.967 | 347 | 5.434 |
| DCM | 10 | 690, 621 | 5.641, 4.984 | 313 | 5.525 |
| DMSO | 10 | 681, 642 | 5.435, 5.329 | 342 | 5.586 |

0.30 ml of DMF was added to this reaction mixture, and then the mixture was heated in the sealed glass tube for 20 min under dry N₂ atmosphere at 320 °C. After cooling to room temperature, 3 mL of DMF was added to the residue to solve the product. The reaction mixture was precipitated by adding acetic acid. The precipitate was filtered and washed with hot acetic acid, water, ethanol and acetonitrile for 12 h in the soxhlet apparatus respectively. The crude product was purified by column chromatography with silica gel eluting with chloroform a gradient of chloroform-THF from 0 to 5% THF.

2.3.3.1. *2(3),9(10),16(17),23(24)-Tetrachloro-3(2),10(9),17(16),24(23)-tetrakis(4-(4-methoxyphenyl)-8-methylcoumarin-7-yloxy)phthalocyaninato cobalt(II) 6.* The compound **6** was obtained and purified as explained by the procedure given above for synthesis of metal Pcs. It is soluble in toluene, DCM, chloroform, THF, DMF and DMSO. Mp > 350 °C. Yield: 101.2 mg (74.26%). Anal. Calc. for C₁₀₀H₆₀Cl₄CoN₈O₁₆: C, 65.62, H, 3.30; N, 6.12. Found: C, 65.85; H, 3.15; N, 5.97%. IR (KBr pellet) ν_{\max} (cm⁻¹): 533, 742, 758, 837, 865, 901, 960, 1042, 1086, 1178, 1250, 1278, 1251, 1368, 1415, 1455, 1488, 1513, 1603, 1731, 2865, 2926, 2960. MALDI-TOF mass m/z : 1827.334 (M)⁺ and 1850.125 (M+Na)⁺. UV-Vis (DCM): λ_{\max} (nm), (log ϵ): 315 (2.573), 610 (4.830), 678 (5.504).

2.3.3.2. *2(3),9(10),16(17),23(24)-Tetrachloro-3(2),10(9),17(16),24(23)-tetrakis(4-(4-methoxyphenyl)-8-methyl-coumarin-7-yloxy)phthalocyaninato zinc(II) 7.* The compound **7** was obtained and purified as explained by the procedure explained above. This compound is soluble in toluene, DCM, chloroform, THF, DMF, DMA and DMSO. Mp > 300 °C. Yield: 95.15 mg (69.82%). Anal. Calc. for C₁₀₀H₆₀Cl₄N₈O₁₆Zn: C, 65.39; H, 3.29; N, 6.10. Found: C, 65.61; H, 3.11; N, 5.93%. IR (KBr pellet) ν_{\max} (cm⁻¹): 527, 566, 604, 743, 829, 864, 944, 1024, 1042, 1084, 1114, 1175, 1247, 1366, 1393, 1422, 1469, 1512, 1595, 1724, 2838, 2933, 3068. MALDI-TOF mass m/z : 1832.486 (M)⁺ and 1855.528 (M+Na)⁺, 1871.712 (M+K)⁺. UV-Vis (DCM): λ_{\max} (nm), (log ϵ): 336 (5.343), 614 (5.024), 690 (5.568). ¹H NMR (CDCl₃), δ , ppm: 7.80–7.04 (m, 36H, Ar-H), 3.85 (s, 12H, CH₃-O), 2.61 (s, 12H, CH₃-).

2.3.3.3. *2,3,9,10,16,17,23,24-Octakis(4-(4-methoxyphenyl)-8-methyl-coumarin-7-yloxy)phthalocyaninato cobalt(II) 9.* A blue-green reaction product **9** was obtained and purified as explained by the pro-

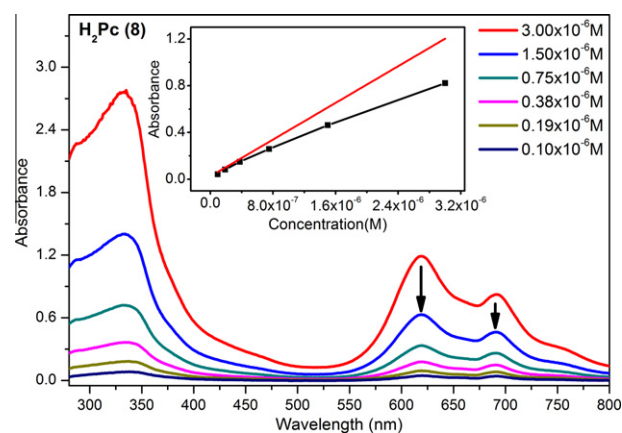


Fig. 3. The UV-Vis spectra of **8** in the range of 3×10^{-6} – 1.0×10^{-7} mol dm $^{-3}$ in DMSO. The inset shows the plot of absorbance vs. concentration.

cedure given above. Compound **9** is soluble in toluene, DCM, chloroform, THF, DMF, DMA and DMSO. Mp > 350 °C. Yield: 40 mg (38.10%). Anal. Calc. for C₁₆₈H₁₁₂CoN₈O₃₂: C, 71.71; H, 4.01; N, 3.98. Found: C, 71.55; H, 3.86; N, 4.21%. IR (KBr pellet) $\nu_{\max}/\text{cm}^{-1}$: 533, 687, 751, 836, 886, 1088, 1109, 1178, 1255, 1367, 1403, 1439, 1513, 1598, 1731, 2930, 2957. MALDI-TOF mass m/z : 2811.444 (M)⁺ and 2834.659 (M+Na)⁺. UV-Vis (DCM): λ_{\max} (nm), (log ϵ): 312 (5.610), 612 (5.113), 676 (5.605).

2.3.3.4. *2,3,9,10,16,17,23,24-Octakis(4-(4-methoxyphenyl)-8-methyl-coumarin-7-yloxy)phthalocyaninato zinc(II) 10.* The compound **10** was obtained and purified as explained by the procedure given above. This compound is soluble in toluene, DCM, chloroform, THF, DMF, DMA and DMSO. Mp > 300 °C. Yield: 58.23 mg (55.46%). Anal. Calc. for C₁₆₈H₁₁₂N₈O₃₂Zn: C, 71.55; H, 4.00; N, 3.97. Found: C, 71.44; H, 3.89; N, 4.11%. IR (KBr pellet) ν_{\max} (cm⁻¹): 531, 615, 742, 833, 863, 884, 990, 1024, 1079, 1176, 1245, 1366, 1389, 1422, 1486, 1511, 1596, 1721, 2836, 2936, 2930, 3068. MALDI-TOF mass m/z : 2816.547 (M)⁺, 2839.669 (M+Na)⁺ and 2855.621 (M+K)⁺. UV-Vis (DCM): λ_{\max} (nm), (log ϵ):

Table 2
Voltammetric data on Pt for **8–10**.

| Complex | Electrolyte | Ring oxidations | M ^{II} /M ^{III} | M ^{II} /M ^I | Ring reductions | Substituent reduction | $E_{1/2}$ | Reference | | |
|---|-------------|-------------------------------|-----------------------------------|---------------------------------|-----------------|-----------------------|--------------|-----------|------|----|
| ^a 8 (H ₂ Pc) | DMSO/TBAP | ^d $E_{1/2}$ (V) | | | -0.51 | -0.97 | | tw | | |
| | | ^e ΔE_p (V) | | | 0.060 | 0.100 | | | | |
| ^b BS-H ₂ Pc | DMSO/TBAP | ^d $E_{1/2}$ (V) | | | -0.56 | -0.88 | | 31 | | |
| | | ^e ΔE_p (V) | | | 0.090 | 0.080 | | | | |
| ^a 9 (CoPc) | DCM/TBAP | ^d $E_{1/2}$ (V) | 0.77 | 1.20 | -0.19 | -0.84 | -1.11 | -1.58 | 0.96 | tw |
| | | ^e ΔE_p (V) | 0.100 | - | 0.060 | - | 0.100 | - | - | |
| | DMSO/TBAP | ^d $E_{1/2}$ (V) | | 0.35 | -0.41(-0.65) | -1.25 | - | -1.84 | 0.76 | tw |
| | | ^e ΔE_p (V) | | 0.100 | 0.100 | - | - | - | - | |
| ^b BS-CoPc | DMSO/TBAP | ^d $E_{1/2}$ (V) | | 0.35 | -0.31 | -1.24 | - | -1.63 | 0.66 | 31 |
| | | ^e ΔE_p (V) | | 0.060 | 0.060 | 0.100 | 0.220 | - | - | |
| ^a 10 (ZnPc) | DCM/TBAP | ^d $E_{1/2}$ (V) | 1.13 | 0.65 | -0.71 | -1.01 | -1.63 | - | 1.36 | tw |
| | | ^e ΔE_p (V) | - | 0.080 | 0.080 | 0.060 | 0.200 | - | - | |
| | DMSO/TBAP | ^d $E_{1/2}$ (V) | 0.81 (0.91) | | | -0.50 (-0.63) | -0.91(-1.19) | -1.62 | 1.31 | tw |
| | | ^e ΔE_p (V) | | | | 0.100 | 0.060 | 0.14 | - | |
| ^b BS-ZnPc | DMSO/TBAP | ^d $E_{1/2}$ (V) | 1.06 | 0.96 | -0.55 (-0.70) | -0.81 (-1.07) | -1.65 | - | 1.51 | 31 |
| | | ^e ΔE_p (V) | | | | 0.060 | 0.200 (0.18) | 0.200 | - | |

^a Octa-4-(4-methoxyphenyl)-7-oxo-8-methylcoumarin- substituted phthalocyanine, reported in this study.

^b Previously reported beta-7-oxy-4-(4-methoxyphenyl)-8-methylcoumarin substituted phthalocyanine.

^c The redox behaviour of the compounds in DMSO/TBAP was complicated by aggregation phenomenon and thus, some redox couples were split.

^d $E_{1/2} = (E_{pa} + E_{pc})/2$ at 0.050 V s^{-1} .

^e $\Delta E_p = E_{pa} - E_{pc}$ (usually at 0.050 V s^{-1}).

^f $\Delta E_{1/2} = E_{1/2}$ (first oxidation) - $E_{1/2}$ (first reduction).

313 (5.525), 621 (4.984), 690 (5.641). ¹H NMR (CDCl₃), δ , ppm: 7.60–6.80 (m, 64H, Ar-H), 3.74 (s, 24H, CH₃-O), 2.36 (s, 24H, CH₃).

2.4. Electrochemistry

The cyclic and differential pulse voltammetry measurements were carried out with a PAR VersoStat II Model potentiostat/galvanostat controlled by an external PC and utilizing a three-electrode configuration at 25 °C. The working electrode was a Pt plate with a surface area of 0.10 cm². A Pt wire served as the counter electrode. Saturated calomel electrode (SCE) was employed as the reference electrode and separated from the bulk of the solution by a double bridge. Electrochemical grade tetrabutylammonium perchlorate (TBAP) in extra pure DMSO or DCM was employed as the supporting electrolyte at a concentration of 0.10 mol dm⁻³. High purity N₂ was used for deoxygenating the solution at least 20 min prior to each run and to maintain a nitrogen blanket during the measurements. *In situ* spectroelectrochemical measurements were carried out by an Agilent Model 8453 diode array spectrophotometer equipped with the potentiostat/galvanostat and utilizing an optically transparent thin layer cell with three-electrode configuration at 25 °C. The working electrode was transparent Pt gauze. Pt wire counter electrode and a SCE reference electrode separated from the bulk of the solution by a double bridge were used.

3. Results and discussion

3.1. Synthesis and characterization

Octa-substituted Pcs bearing eight 4-(4-methoxyphenyl)-7-oxo-8-methylcoumarin substituents **8–10** and four chloro substituents in addition to four 4-(4-methoxyphenyl)-7-oxo-8-methylcoumarin substituents **5–7** were synthesized and characterized to investigate differences in their spectroscopic and aggregation behaviours. 4,5-dichlorophthalonitrile (**1**) and 7-hydroxy-4-(4-methoxyphenyl)-8-methylcoumarin (**2**) have been synthesized by the method in the literature [35,36]. Unfortunately, despite our all efforts, the reaction between **1** and **2** produced a mixture of **3** and **4** rather than the single product of **3** or **4**. For this reason, the compounds **3** and **4** in the reaction mixture were separated by column chromatography. Compounds **5–7** and **8–10** were synthesized by using the new pure

starting compounds **3** and **4**, respectively (Scheme 1). In fact, the phthalocyanine product **5**, **6** or **7** was a mixture of its positional isomers due to the involvement of two different substituents (chlorine and coumarine derivative) in the phthalonitrile precursor. The photophysical and electrochemical data of the relevant compounds were obtained from the measurements performed on the mixtures of their isomers.

The characterization of the new products involved a combination of methods including The IR, UV-Vis, ¹H NMR and MALDI-TOF mass spectrometry and elemental analyses. The results are consistent with the proposed structures.

The formation of starting compounds was confirmed clearly by the appearance of the new absorption bands at 2232 cm⁻¹ (-C≡N) and 1280 cm⁻¹ (Ar-O-Ar) for **3**, and at 2235 cm⁻¹ (-C≡N) and 1292 cm⁻¹ (Ar-O-Ar) for **4** in their FT-IR spectra. Compounds **3** and **4** exhibited -C=C- double bond at 1603 and 1604 cm⁻¹, coumarin carbonyl (lactone, -C=O) at 1720 and 1713 cm⁻¹, -CH₃ at 2838;2930 and 2838;2931 cm⁻¹ and Ar-H stretching frequencies at 3070 and 3041 cm⁻¹ respectively. The FT-IR spectra of Pcs **5–10** showed Ar-O-Ar, =C=C-, -C=O, -C≡N, -CH₃ and aromatic -CH-peaks within the ranges of 1220–1285, 1560–1655, 1760–1780,

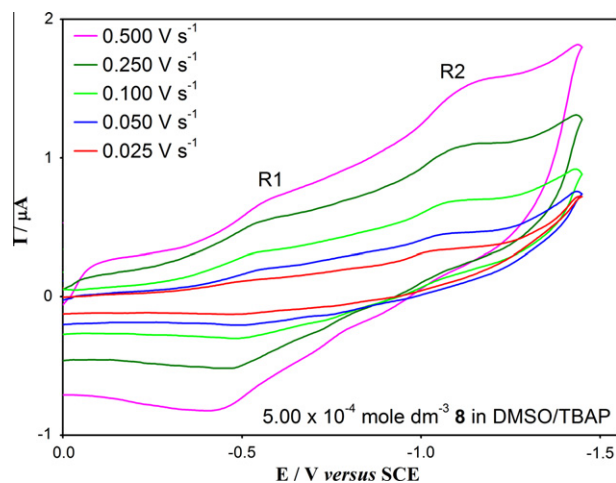


Fig. 4. Cyclic voltammograms of $5.0 \times 10^{-4} \text{ mol dm}^{-3}$ **8** in DMSO/TBAP.

1670–1720, 2800–2980 and 3060–3080 cm^{-1} , respectively. The IR-spectra of the Pcs are very similar, with the exception of metal-free Pcs **5** and **8**, showing a N–H weak stretching band due to the inner core at 3298, 3289 cm^{-1} respectively. In addition, disappearing of $-\text{C}\equiv\text{N}$ peaks at 2232–2235 cm^{-1} clearly indicated that starting compounds **3** and **4** were converted to the Pcs **5–10**.

The ^1H NMR spectra of **3** and **4** showed characteristic signals for methyl ($-\text{CH}_3$) protons at δ 2.20 ppm and methoxy ($-\text{OCH}_3$) protons at δ 3.75 and 3.74 ppm each a singlet, respectively. The peaks within the ranges of 6.71–7.15 and 6.70–7.33 ppm indicated the presence of the aromatic protons in compounds **3** and **4**, respectively (Supplementary Materials, Figs. S1 and S2). The ^1H NMR spectra of the Pc compounds **5**, **7**, **8** and **10** were almost identical with those of the starting phthalonitrile compounds **3** and **4**, except broadening and small shifts in the peaks of the formers. The ^1H NMR spectra of **5**, **7**, **8** and **10** showed aromatic protons signals within the ranges of 7.73–6.98 ppm for **5**, 7.80–7.04 ppm for **7**, 7.74–6.92 ppm for **8**, and 7.60–6.80 ppm for **10** and aliphatic protons signals within the range of 3.85–2.27 ppm ($-\text{OCH}_3$ and $-\text{CH}_3$) for **5**, **7**, **8** and **10**, as expected (Supplementary Materials, Figs. S3–S6).

The ^{13}C NMR signals for aromatic and aliphatic ($-\text{OCH}_3$ and $-\text{CH}_3$) carbon atoms appeared within the range of 161.04–110.47 ppm, at 55.65 ppm, and at 9.26 ppm for **3** and within the range of 160.95–111.35 ppm, at 55.48 ppm and at 9.00 ppm for **4**, respectively (Supplementary Materials, Figs. S7 and S8).

The UV–Vis spectra of Pcs **5–10** in various solvents (DMSO, DCM, toluene and chloroform) showed characteristic Q band absorptions around 656–705 nm which were attributed to the $\pi \rightarrow \pi^*$ transitions from the highest occupied molecular orbital (HOMO) to the lowest unoccupied molecular orbital (LUMO) of the Pc ring. The other B bands in the UV range 288–352 nm were due to transitions from the deeper π levels to the LUMO (Fig. 1).

In MALDI-TOF-MS spectra, the molecular ion peaks of **5–10** were observed at 1770.025, 1827.334, 1832.486, 2754.573, 2811.444 and 2816.547 Da, respectively (Fig. 2). Beside the molecular ion peaks of the complexes, sodium ion adducts were also observed. In addition, potassium ion adducts were only observed in the spectra of zinc Pcs (**7** and **10**). The complexes showed low fragmentation under the MALDI-TOF-MS conditions in reflectron mode. All high resolved experimental peaks matched perfectly the theoretical peaks of the complexes determined by isotropic software calculation. Thus, MS analyses confirmed the molecular formula of all Pc samples.

3.2. Spectral properties

The Q and B-band absorption data of **5–10** in different solvents are summarized in Table 1. The split Q-band absorptions of metal-free Pcs have been observed at 673 and 704 nm, 674 and 705 nm, and 669 and 701 nm for **5** and at 668 and 702 nm, 665 and 700 nm, and 665 and 699 nm for **8** in toluene, chloroform and DCM, respectively (Fig. 1A and B). D_{2h} symmetry of **8** causes the splitting of its Q-band absorptions. Its split Q-band absorption in non-coordinating solvents toluene, chloroform and DCM can be attributed to $\pi-\pi^*$ electronic transitions of its monomeric species, but not to the aggregated species. There are also vibrational absorptions as two shoulders in its spectrum in the mentioned solvents. The UV–Vis spectrum of **8** in DMSO involves a broad and weak non-split Q-band absorption at 691 nm, in addition to a broad and relatively much stronger absorption at 619 nm, and the B-band at 334 nm as a single peak (Fig. 1B).

The UV–Vis spectra of **6**, **7**, **9** and **10** in non-coordinating solvents toluene, chloroform and DCM exhibit sharp and non-split Q-band absorptions within the range of 671–690 nm which are characteristic for monomeric metal Pcs. Their vibrational absorp-

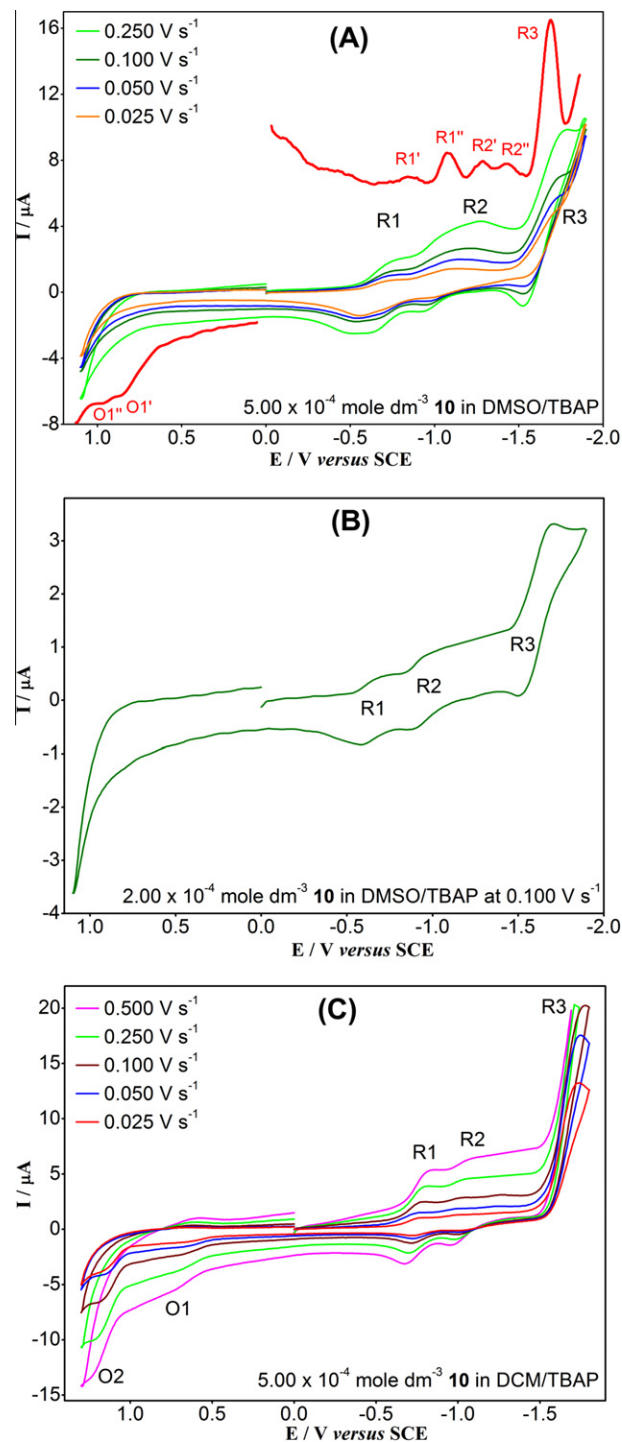


Fig. 5. Cyclic voltammograms of (A) $5.0 \times 10^{-4} \text{ mol dm}^{-3}$ (B) $2.0 \times 10^{-4} \text{ mol dm}^{-3}$ **10** in DMSO/TBAP and (C) $5.0 \times 10^{-4} \text{ mol dm}^{-3}$ **10** in DCM/TBAP. The dotted lines in (A) displays differential puls voltammogram of $5.0 \times 10^{-4} \text{ mol dm}^{-3}$ **10** in DMSO/TBAP.

tions and B-bands appear within the range of 607–621 and 309–352 nm, respectively (Fig. 1C–F and Table 1). However, these complexes display broad or split absorptions in the Q-band region in DMSO, due to the formation of their aggregated species in this solvent. The comparison of the molar absorptivity of **6** and **7** with those of **9** and **10** shows that the formers involving eight oxy-coumarin substituents have lower molar absorptivity than the latter with four oxy-coumarin substituents and four chlorine atoms

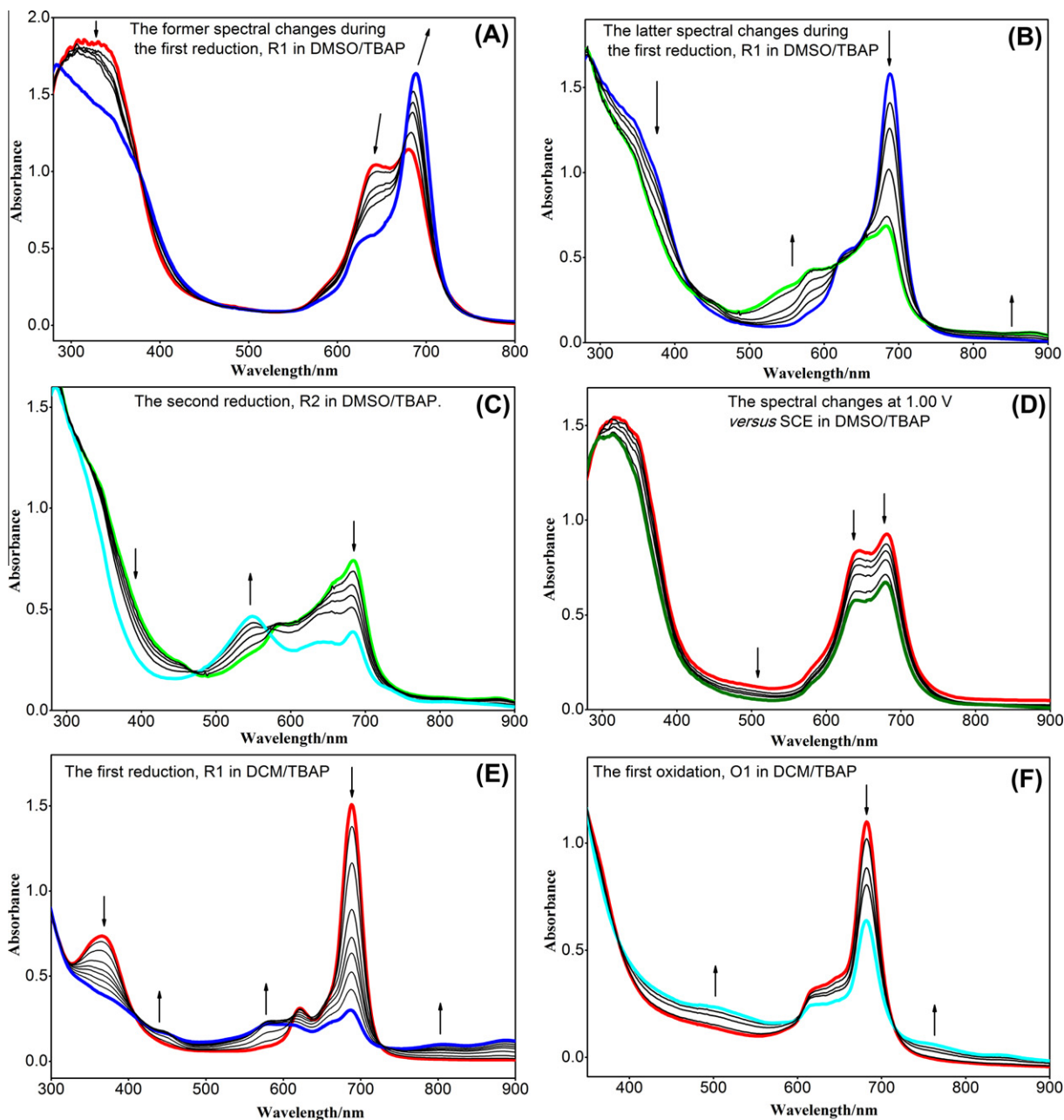


Fig. 6. *In situ* UV-Vis spectral changes during controlled-potential electrolysis of **10** in DMSO /TBAP or DCM/TBAP.

(Table 1). This comparison indicates that the aggregation tendencies of the latters are higher than those of the formers, due to the increasing intermolecular interactions as a result of the increase in the number of more electron-withdrawing oxy-coumarin substituents.

Aggregation behaviour of **5–10** was also examined by the spectra monitored at different concentrations in DMSO with the aim of providing additional support for the formation of their aggregated species in this solvent. In general, the decrease in the absorptions of the blue shifted broad bands was more pronounced than that of the main Q-band corresponding monomeric species. The spectra of **8** at different concentrations in DMSO within the range between 3×10^{-6} and 1.0×10^{-7} mol dm $^{-3}$ are shown in Fig. 3 as a typical example. As the concentration of **8** is decreased, the decrease in the absorption for the band at 619 nm is more pronounced than that for the main Q-band and thus, their intensities become approxi-

mately equal at the concentration of 0.10×10^{-6} mol dm $^{-3}$. This observation provides strong evidence for the assignment of the band at 619 nm to the H-type aggregates. The aggregation phenomenon was also tested by the change of absorbance with concentration within the range of 3.0×10^{-6} to 1.0×10^{-7} mol dm $^{-3}$ in DMSO. The presence of aggregated species was confirmed by the deviation from Beer–Lambert law (inset in Fig. 3) [37].

The term solvatochromism is used to describe the pronounced change in position (and sometimes intensity) of the UV-Vis absorption band, that accompanies a change in the polarity of the medium. A hypsochromic (or blue) shift with increasing solvent polarity is usually named negative solvatochromism, while the positive solvatochromism corresponds to a bathochromic (or red) shift [38]. Solvent effects on UV-Vis absorption bands of the Pcs was studied in several solvents with different polarities (toluene < DCM < chloroform < DMSO). When UV-Vis spectra of

CoPcs (**6** and **9**) and ZnPcs (**7** and **10**) in DMSO (as a polar solvent) compared with in non-polar solvents, 14–17 nm and 7–9 nm the blue shift were observed respectively. On the other hand, Q absorption bands of metal free Pcs **5** and **8** were shifted 9–12 nm to red (Fig. 1 and Table 1).

When the spectrum Pcs **5–7** bearing two different substituents (Cl and oxy-coumarin) compared with Pcs **8–10** bearing only one type of substituent (oxy-coumarin), it was observed that the Q band of the **8** and **9** were blue-shifted approximately 5 nm according to **5** and **6** but **10** were red-shifted approximately 2 nm according to **7**. These UV–Vis spectra show that peripheral substituents of Pcs **5–10** affect their spectral properties weakly (Fig. 1 and Table 1).

3.3. Electrochemistry

The electrochemical behaviour of octa-4-(4-methoxyphenyl)-7-oxo-8-methylcoumarin- substituted Pcs **8–10** was investigated by cyclic voltammetry, differential pulse voltammetry and *in situ* spectroelectrochemistry in DMSO and DCM involving tetrabutylammonium perchlorate (TBAP) as supporting electrolyte. The voltammetric data of the complexes, including the half-wave redox potential value ($E_{1/2}$), anodic-to-cathodic peak potential separation (ΔE_p) and the difference between the first oxidation and reduction potential ($\Delta E_{1/2}$) are summarized in Table 2 which also includes the data for recently reported tetra-substituted analogues of **8–10** for comparison.

Compound **8** displayed two reduction couples (R1 and R2) within the available potential range in DMSO/TBAP (Fig. 4). These processes are clearly Pc ring-based since compound **8** is metal-free. As observed previously for tetra-substituted analogue of **8** [37], the first oxidation process of **4** is out of the accessible potential range of DMSO/TBAP medium, probably as a result of the stabilization of the HOMO and the LUMO, and thus, shifting the redox potentials towards more positive potentials by 4-(4-methoxyphenyl)-7-oxo-8-methylcoumarin substituents. Similarly, both cathodic and anodic waves of the first and the second reduction couples (R1 and R2) of **8** are broad which can be attributed to the presence of its aggregated species and equilibrium between monomeric and aggregated species. However, as shown in Table 2, the first reduction process of **8** occurs at a potential ($E_{1/2} = -0.51$ V) somewhat less negative than that ($E_{1/2} = -0.56$ V) of its tetra-substituted analogue [37]. The separation between the first and second ring reductions is approximately 0.46 V, which is in agreement with the reported ones for redox processes in metal-free Pcs [39]. The redox potentials of **8** are less negative than those of the previously reported [39] unsubstituted metal-free Pcs in a similar coordinating solvent, DMF, due to electron withdrawing nature of 4-(4-methoxyphenyl)-7-oxo-8-methylcoumarin substituents, suggesting that the redox potentials of Pcs can be changed remarkably by peripheral substituents.

Fig. 5A shows the cyclic and differential pulse voltammograms of 5.00×10^{-4} mol dm⁻³ solution of **10** in DMSO/TBAP at different scan rates. It shows three reduction processes (R1–R3) and an oxidation couple (O1). As shown in Fig. 5A, the first and second reduction couples are remarkably broad. The oxidation process (O1) could be identified only by DPV, due to its high positive potential within the available potential range. Furthermore, R1, R2 and O1 processes are split on the differential pulse voltammogram of **10**. When the concentration of the compound was changed from 5.00×10^{-4} mol dm⁻³ to 2.00×10^{-4} mol dm⁻³, the broadness of the R1 and R2 decreased considerably (Fig. 5B). All these observations indicates clearly that the electron transfer processes of **10** in DMSO/TBAP are associated by the equilibrium between aggregated and deaggregated species. The π – π^* interactions between the π -electron clouds of adjacent Pc macrocycles as a result of their coplanar association is called as aggregation. This phenomenon results generally in broadening of the redox signals or their splitting, due to the differences

in the redox potentials of aggregated and deaggregated species. The peripheral nature of the substituents in beta-substituted Pcs, leading to the planarity should be the main reason for the high aggregation tendency of these compounds. Fig. 5C shows the cyclic voltammograms of 5.00×10^{-4} mol dm⁻³ solution of **10** in DCM/TBAP at different scan rates. It also displays three reduction (R1–R3) processes, but two oxidation couples (O1 and O2) due to relatively wide positive potential range available, compared to that in DMSO/TBAP. The redox couples of **10** in DCM/TBAP are neither broad nor split which shows the absence of aggregated species. The R4 couple, appearing at high negative potentials at the end of solvent-limited cathodic potential range in DMSO/TBAP and DCM/TBAP, should correspond to the reduction of 4-(4-methoxyphenyl)-7-oxo-8-methylcoumarin substituents since these groups, less conjugated as compared with the Pc ring are expected to be reduced at relatively high negative potentials. Anyway, the redox-active nature of oxy-coumarin substituents in Pc compounds has been reported previously [37,40]. It is clear from the well-known redox-inactive nature of metal center in zinc Pcs, other redox processes in DMSO/TBAP and DCM/TBAP (R1, R2, O1 and O2) can be attributed to successive addition of electrons to, and removal of an electron from the Pc ring [39]. However, *in situ* spectroelectrochemical measurements were carried out during the controlled potential electrolysis of **10** in DMSO at a suitable potential corresponding to its first reduction process since this type of measurements do not only have a vital importance in determining the nature of the redox processes, but also provide

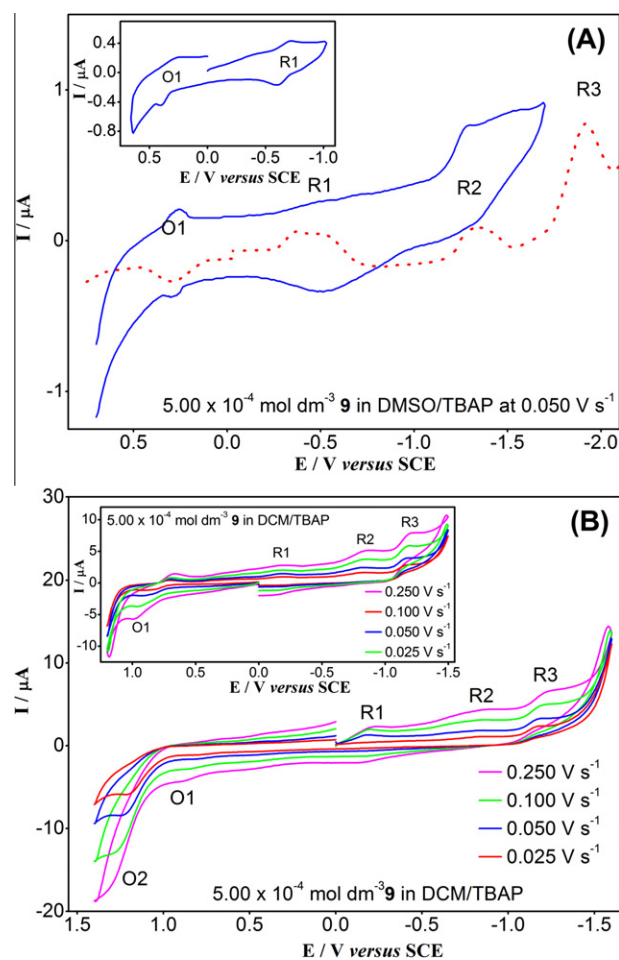


Fig. 7. Cyclic voltammograms of 5.0×10^{-4} mol dm⁻³ **9** in (A) DMSO/TBAP (B) DCM/TBAP. The dotted lines in (A) displays differential pulse voltammogram of 5.0×10^{-4} mol dm⁻³ **9** in DMSO/TBAP. The insets in (A) and (B) shows the cyclic voltammograms monitored with different switching potentials.

support for the evaluation of the aggregation effect on the redox processes. Fig. 6A and B show the two groups of *in situ* spectroelectrochemical changes, each of which associated with different isosbestic points, during the controlled-potential electrolysis of the solution of **10** in DMSO/TBAP at -0.80 V versus SCE. In Fig. 6A, the Q-band absorption in the spectrum at the start of the electrolysis is split, although the spectroelectrochemical measurements were carried out at relatively low concentrations (1.00×10^{-4} mol dm $^{-3}$) as compared to that in voltammetric measurements (5.00×10^{-4} mol dm $^{-3}$). Therefore, it can be concluded that there is still aggregation–deaggregation equilibrium with the high energy band at 640 nm being due to the aggregate and the low energy band at 680 nm due to the monomer. Upon reduction at -0.80 V versus SCE, the absorption of the aggregation band at 640 nm, decreases while that of the monomer band at 680 nm increases with red shift to 688 nm, as a first group of spectral changes (Fig. 6A). These spectral changes, characteristic for Pc-ring reduction, are followed by a decrease in the monomer band without shift and the formation of a new band at 583 nm (Fig. 6B). The two groups of subsequent spectral changes with different isosbestic points indicate clearly that aggregation–deaggregation equilibrium shifts towards to monomer species before the ligand-based first reduction process. The spectral changes monitored during the second reduction process (R2) at -1.30 V versus SCE, the decrease in the Q-band absorption and the formation of a new band at 548 nm, correspond to the reduction of singly-reduced monomer species (Fig. 6C). Although the O1 process of **10** could be monitored with differential pulse voltammetry, decomposition of the complex, evidenced by the decrease in the

absorption of all bands, occurred during the electrolysis of its solution in DMSO/TBAP at 0.98 V versus SCE, instead of the characteristic spectral changes for this process (Fig. 6D). The UV–Vis spectra, monitored at the beginning of both its first reduction (Fig. 6E) and the first oxidation (Fig. 6F) of **10** in DCM/TBAP at suitable potentials are not broad or split, suggesting clearly that it does not form aggregated species in DCM/TBAP, as also implied by the cyclic voltammograms recorded in this medium (Fig. 5C). The spectral changes in Figs. 6E and F, the decrease in the Q-band absorption without shift and the appearance of a new band within the range of 500–600 nm, are characteristic for Pc-ring-based redox processes [41,42].

The cyclic and differential pulse voltammograms of **9** in DMSO/TBAP are shown in Fig. 7A, which involves three reductions (R1, R2 and R3) and an oxidation (O1) within the available potential range. The comparison of the two cyclic voltammograms in Fig. 7A suggests that the shape of the R1 couple is strongly affected by the switching potential at the cathodic side. The R3 couple could be monitored only by differential pulse voltammetry. The redox signals of **9** in DMSO/TBAP are split or broad which leads to ill-defined voltammograms. This is probably due to the presence of aggregated species. The aggregated species are expected to reduce or oxidize at different potentials in comparison with the deaggregated species, causing the splitting or broadening of the redox signals. The difference between the half-peak potentials of the first oxidation and reduction potentials, $\Delta E_{1/2}$, of **9** is 0.76 V which is much lower in comparison with that of **10**. Thus, it is reduced and oxidized more easily than **10**. This distinctive behaviour of **9** can be attributed to the fact that Co(II) center has accessible d orbital levels lying

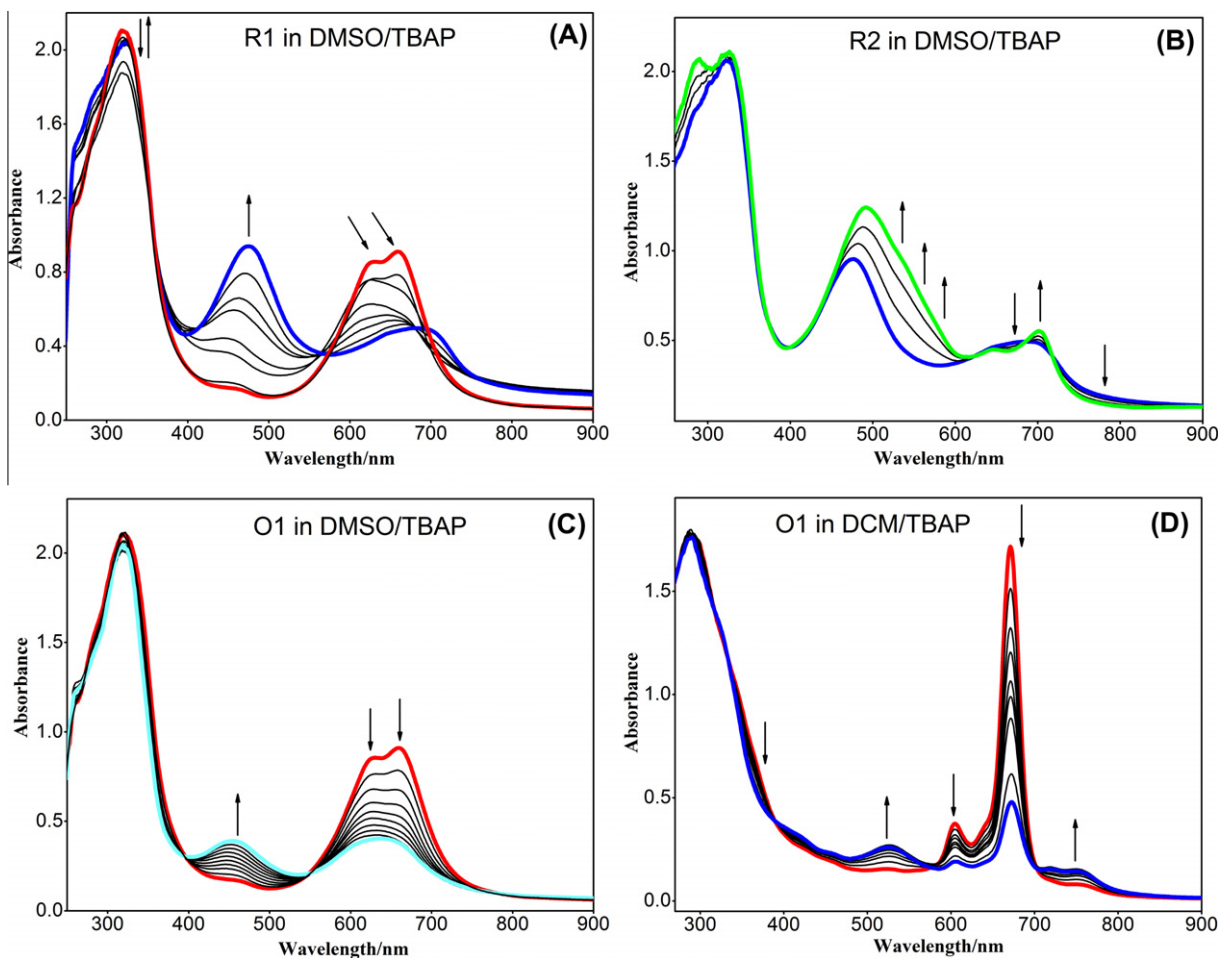


Fig. 8. *In situ* UV–Vis spectral changes during controlled-potential electrolysis of **9** in DMSO/TBAP or DCM/TBAP.

between the HOMO and the LUMO gap of the Pc species. In that case, metal center can be oxidized and reduced before the ring-based redox processes. This type of Pc complexes can vary their electrochemical behaviour according to their environment, depending on whether there are any available coordinating species that would stabilize the Co(II) center. The main difference lies in whether the metal or the ring is oxidized first. Donor solvents strongly favour Co(III)Pc(-2) by coordinating along the axis to form six coordinate species. If such solvents are absent, then oxidation to Co(III) is inhibited and ring oxidation occurs first. Thus, the first oxidation and the first reduction processes of **9** in DMSO/TBAP are probably metal-based and correspond to Co(II)Pc(-2)/[Co(III)Pc(-2)]⁺ and Co(II)Pc(-2)/[Co(I)Pc(-2)]⁻ redox couples, respectively. On the other hand, it is also well known from the literature that the second reduction process is ring-based [39]. The peak currents of the last reduction couple are much higher than those of the other redox couples, as observed also for **10**. This behaviour implies that it corresponds to the reduction of four oxy-coumarin substituents. Spectroelectrochemical measurements were also carried out to assign especially the first reduction and the first oxidation processes of **9** certainly. Fig. 8A shows *in situ* UV–Vis spectral changes during the first reduction of **9** at -0.80 V versus SCE, corresponding to the redox process labelled R1 in Fig. 7A. The split Q-band absorption in the UV–Vis spectrum of **9** in DMSO/TBAP confirms the presence of aggregated species. The band with higher energy corresponds to the aggregated species while the one with lower energy is attributed to the deaggregated species. Upon the first reduction, the absorptions of both bands decrease with red shift, while a new band appears at 475 nm. The new Q-band is considerably broad, suggesting that some singly reduced species are still aggregated after the first reduction process. The spectral changes form various isosbestic points at different wavelengths within the ranges of 683–713 nm and 563–573 nm, rather than the ones at specific wavelengths, due to the formation of different reduced species produced from reduction of aggregated and monomer species of **9**. The band at 475 nm and the shifting of the Q-band indicate the formation of [Co(I)Pc(-2)]⁻ species, confirming the CV assignment of the couple R1 to Co(II)Pc(-2)/[Co(I)Pc(-2)]⁻ process [36–39]. During the second reduction at -1.50 V versus SCE, the higher energy side of the broad Q-band at 687 nm decreases while its lower energy side increases, and thus two new bands appear at 645 and 702 nm. These spectral changes are associated by increase in the absorption within the range of 436–625 and thus, the formation of a band at 492 nm (Fig. 8B). The changes are characteristics for a ring-based reduction in Co(II)Pc complex, and thus, confirm our voltammetric assignment of this process to [Co(I)Pc(-2)]⁻/[Co(I)Pc(-3)]²⁻. Fig. 8C displays *in situ* UV–Vis spectral changes during the first oxidation process at 0.55 V versus SCE. The absorptions of both peaks of the Q-band decrease and a Q-band with the wavelength maximum of 637 nm and a new band at 456 nm appears. The new Q-band is considerably broad, suggesting that some singly oxidized species are still aggregated after the first oxidation process. The formation of a new band at 456 nm is typical of a metal-based oxidation in CoPc complexes and thus, confirms the CV assignment of Co(II)Pc(-2)/[Co(III)Pc(-2)]⁺ for couple O1 of **9** in Fig. 7A [43–46]. The tetra-substituted analogue of **9** did not form aggregated species in DMSO/TBAP, as stated in a recent report [37]. It appears that the increase in the number of peripheral oxy-coumarin substituents increases the extent of cofacial interactions between the neighbouring CoPc molecules, and thus, causes H-type aggregation.

In contrast to its behaviour in DMSO/TBAP, complex **9** shows well-defined redox couples in DCM/TPAP (Fig. 7B), probably due to the absence of aggregated species. The first reduction process (R1) is metal-based and corresponds to Co(II)/Co(I) couple while the other reduction processes are ligand-based [39]. Complex **9** displays two oxidation couples in DCM/TBAP while it shows only

one oxidation couple in DMSO/TBAP within the available potential ranges. Due to the non-coordinating nature of DCM, the first oxidation processes of **9** (O1) is probably ligand-based and corresponds to Co(II)Pc(-2)/[Co(II)Pc(-1)]⁺ couple while the second one (O2) is metal-based and may be attributed to [Co(II)Pc(-1)]⁺/[Co(III)Pc(-1)]²⁺ couple [39]. Fig. 8D displays the UV–Vis spectrum of **9** in DCM/TBAP and *in situ* spectral changes during its first oxidation at 1.05 V versus SCE. The solution of complex **9** in DCM/TBAP does not involve aggregated species as understood clearly from the narrow and nonsplit Q-band at 671 nm in this figure. Upon the first oxidation, the absorptions of the sharp Q band at 671 nm and the vibrational band at 604 nm decreases without shift and two new Q bands at 526 and 755 nm develops. These spectral changes are characteristic for a Pc-based oxidation and thus, lead to the formation of [Co(II)Pc(-1)]⁺ species [41,42]. Unfortunately, the electrolysis of **9** at the potentials more positive than 1.10 V versus SCE in DCM/TBAP resulted in decomposition of the complex, as evidenced from decrease in the absorption of all peaks.

4. Conclusions

The novel metal-free Pcs **5**, **8** and metal Pcs **6**, **7**, **9** and **10** have been prepared from 4-chloro-5-(4-(4-methoxyphenyl)-8-methylcoumarin-7-yloxy)phthalonitrile (**3**) and 4,5-bis(4-(4-methoxyphenyl)-8-methylcoumarin-7-yloxy)phthalonitrile (**4**). The compounds were characterized by UV–Vis, IR and MALDI-TOF mass spectrometry, and elemental analysis. The effect of substituent (the coumarin and chloro), metal (Co and Zn), solvent (DMSO, DCM, toluene and chloroform) and concentration on the spectroscopic properties and aggregation behaviour of the novel compounds were investigated. The compounds displayed high aggregation tendency in DMSO whereas their aggregated species were not observed in DCM, toluene and chloroform. The compounds **8**–**10** showed redox processes located at the ring and/or metal centre. The aggregation character of the compounds in DMSO was reflected by splitting or broadening of the redox waves while the compounds displayed well-defined voltammograms in DCM, due to the absence of aggregated species in this solvent. Furthermore, the nature of the redox processes and the effect of aggregation on the electron transfer processes were identified by *in situ* spectroelectrochemical measurements during controlled-potential electrolysis of the complexes at suitable potentials.

Acknowledgments

We are thankful to The Foundation of Marmara University, The Commission of Scientific Research (BAPKO) (Project No: FEN-A-090909-0302 and FEN-C-DRP-080410-0091) and Turkish Academy of Sciences (TUBA).

Appendix A. Supplementary data

Supplementary data associated with this article can be found, in the online version, at <http://dx.doi.org/10.1016/j.poly.2012.08.080>.

References

- [1] M. Calvete, M. Hanack, Eur. J. Org. Chem. (2003) 2080.
- [2] J. Steven, C. Gorrler-Walrand, K. Binnemas, Mater. Sci. Eng., C 18 (2001) 229.
- [3] S.M. Gorun, J.W. Rathke, M.J. Chen, Dalton Trans. (2009) 1095.
- [4] M.R. Christie, B.G. Freer, Dyes Pigm. 24 (1994) 113.
- [5] M. Özer, A. Altındal, A.R. Özkaya, Ö. Bekaroğlu, Dalton Trans. 17 (2009) 3175.
- [6] Y. Açıkbaz, M. Evyapan, T. Ceyhan, R. Çapan, Ö. Bekaroğlu, Sens. Actuators, B 135 (2009) 426.
- [7] A. Wang, L. Long, C. Zhang, J. Incl. Phenom. Macrocycl. Chem. 71 (2011) 1.
- [8] T. Goslinska, J. Piskorz, J. Photochem. Photobiol., C 12 (2011) 304.
- [9] M. Pişkin, M. Durmuş, J. Photochem. Photobiol., A 223 (1) (2011) 37.

- [10] G.A. Gaunaa, J. Marinob, M.C.G. Viora, L.P. Roguinb, J. Awrucha, *Eur. J. Med. Chem.* 46 (11) (2011) 5532.
- [11] J. Marino, M.C.G. Vior, L.E. Dicalio, L.P. Roguin, J. Awruch, *Eur. J. Med. Chem.* 45 (9) (2010) 4129.
- [12] T. Goslinski, T. Osmalek, K. Konopka, M. Wierzchowski, P. Fita, J. Mielcarek, *Polyhedron* 30 (2011) 1538.
- [13] D. Gu, Q. Chen, X. Tang, F. Gan, S. Shen, K. Liu, H. Xu, *Opt. Commun.* 121 (1995) 125.
- [14] M. Yükses, T. Ceyhan, F. Bağcı, H.G. Yağlıoğlu, A. Elmali, Ö. Bekaroğlu, *Opt. Commun.* 281 (2008) 3897.
- [15] B.C. O'Regan, I.L. Duarte, M.V.M. Díaz, A. Forneli, J. Albero, A. Morandeira, E. Palomares, T. Torres, J.R. Durrant, *J. Am. Chem. Soc.* 130 (2008) 2906.
- [16] İ. Koç, M. Özer, A.R. Özkaya, Ö. Bekaroğlu, *Dalton Trans.* 32 (2009) 6368.
- [17] F.H. Moser, A.H. Thomas (Eds.), *The Phthalocyanines*, vols. 1–2, CRC Press, Florida, 1983.
- [18] C.C. Leznoff, A.B.P. Lever (Eds.), *Phthalocyanines Properties and Applications*, vol. 1, VCH Publishers, New York, 1989 (1993, vols. 2–3, 1996, vol. 4.).
- [19] N.B. McKeown, *Phthalocyanine Materials: Synthesis, Structure and Function*, Cambridge Un. Press, 1998.
- [20] K.P. Mahesh, S.M. Swapnil, M.S. Manikrao, *Tetrahedron Lett.* 42 (2001) 9285.
- [21] S.D. Bose, A.P. Rudradas, M.H. Babu, *Tetrahedron Lett.* 43 (2002) 9195.
- [22] D. Sibbing, N.V. Beckerath, T. Morath, J. Stegherr, J. Mehilli, N. Sarafoff, S. Braun, S. Schulz, A. Schömig, A. Kastrati, *Eur. Heart J.* 31 (10) (2010) 1205.
- [23] R. O'Kennedy, R.D. Thornes, *Coumarins: Biology, Applications and Mode of Action*, Wiley & Sons, Chichester, 1997.
- [24] M. Zahradnik, *The Production and Application of Fluorescent Brightening Agents*, Wiley & Sons, 1992.
- [25] R.D.H. Murray, J. Mendez, S.A. Brown, *The Natural Coumarins: Occurrence, Chemistry and Biochemistry*, Wiley & Sons, New York, 1982.
- [26] H. Zhao, N. Neamati, H. Hong, A. Mazumder, S. Wang, S. Sunder, G.W.A. Milne, Y. Pommier, T.R. Burke, *J. Med. Chem.* 40 (2) (1997) 242.
- [27] S.L.J. Michael, A.G.M. Barrett, B.M. Hoffman, *Inorg. Chem.* 42 (2003) 814.
- [28] M.N. Yarasir, M. Kandaz, A. Koca, B. Salih, *Polyhedron* 26 (2007) 1139.
- [29] M. Çamur, A.R. Özkaya, M. Bulut, *Polyhedron* 26 (2007) 2638.
- [30] A.A. Esenpınar, A.R. Özkaya, M. Bulut, *Polyhedron* 28 (2009) 33.
- [31] N. Sheng, R. Li, C. Choi, W. Su, D.K.P. Ng, X. Cui, K. Yoshida, N. Kobayashi, J. Jiang, *Inorg. Chem.* 45 (2006) 3794.
- [32] J. Simon, P. Bassoul, in: C.C. Leznoff, A.B.P. Lever (Eds.), *Phthalocyanines: Properties and Applications*, vol. 2, VCH Publishers, New York, 1993, p. 223.
- [33] D.D. Dominquez, A.W. Snow, J.S. Shirk, R.G.S. Pong, J. Porphyrins *Phthalocyanines* 5 (2001) 582.
- [34] H.S. Nalwa, J.S. Shirk, in: C.C. Leznoff, A.B.P. Lever (Eds.), *Phthalocyanines: Properties and Applications*, vol. 4, VCH Publishers, New York, 1996, p. 79.
- [35] D. Wöhrle, M. Eskes, K. Shigehara, A. Yamada, *Synthesis* (1993) 194.
- [36] M.M. Garazd, Y.L. Garazd, A.S. Ogorodniichuk, V.P. Khilya, *Chem. Nat. Compd.* 38 (2002) 539.
- [37] I. Acar, Z. Biyıklioğlu, M. Durmuş, H. Kantekin, *J. Organomet. Chem.* 708–709 (2012) 65.
- [38] C. Reichardt, *Solvents and Solvent Effects in Organic Chemistry*, Wiley-VCH, Weinheim, 2003.
- [39] A.B.P. Lever, E.R. Milaeva, G. Speier, in: C.C. Leznoff, A.B.P. Lever (Eds.), *Phthalocyanines: Properties and Applications*, vol. 3, VCH Publishers, New York, 1993, pp. 1–69.
- [40] A. Alemdar, A.R. Özkaya, M. Bulut, *Synth. Met.* 160 (2010) 1556.
- [41] J. Mack, M.J. Stillman, *J. Am. Chem. Soc.* 116 (1994) 1292.
- [42] T. Nyokong, Z. Gasyna, M. Stillman, *Inorg. Chem.* 26 (1987) 548.
- [43] Z. Odabaş, A. Altındal, A.R. Özkaya, B. Salih, M. Bulut, Ö. Bekaroğlu, *Polyhedron* 26 (2007) 695.
- [44] M. Özer, A. Altındal, A.R. Özkaya, M. Bulut, Ö. Bekaroğlu, *Polyhedron* 25 (2006) 3593.
- [45] P.C. Martin, M. Gouterman, B.V. Pepich, G.E. Renzoni, D.C. Schindele, *Inorg. Chem.* 30 (1991) 3305.
- [46] M.J. Stillman, A.J. Thomson, *J. Chem. Soc., Faraday Trans. II* (70) (1974) 790.